the models require computation of the inverse Q function. Computation of Q however is significantly less involved than recursively solving (3) and (4). Furthermore, most mathematics software packages include built-in variants of the Q function, such as erfc(x) or erf(x). They often include mechanisms for computing inverses of these functions, as well. Hence, as we see from the results in Figs. 3–6, the radiometer models presented here provide reasonable results, and are significantly easier to use than exact computations.

IV. CONCLUSIONS

Several detection models for the wideband radiometer have been presented. The purpose of these models is to provide a simple means of predicting the required SNR to achieve some desired performance (P_d and P_{fa}). Comparisons with exact results showed that the Torrieri, Engler, EVGA models converge to the exact results for very large time-bandwidth products. For $TW > 1000$ the maximum error using any of the models is less than 0.5 dB.

ROBERT F. MILLS
Department of Electrical and Computer Engineering
Air Force Institute of Technology
Bldg. 640, Suite 218
2950 P Street
Wright-Patterson AFB, OH 45433-7765

GLENN E. PRESCOTT
Department of Electrical Engineering and Computer Science
University of Kansas
Lawrence, KS 66045

REFERENCES

[1] Torrieri, D. J. (1992)
Principles of Secure Communications Systems.
Boston: Artech House, 1992.

[2] Edell, J. D. (1976)
Wideband, noncoherent, frequency-hopped waveforms and their hybrids in low-probability of intercept communications.
Report NRL 8025, Naval Research Laboratory, Washington, DC, Nov. 8, 1976.

[3] Nicholson, D. (1988)
Spread Spectrum Signal Design: LPE and AJ Systems.
Rockville, MD: Computer Science Press, 1988.

[4] Bruce, J. D., and Snow, K. D. (1974)
Final technical report TEAL WING program.
Probe Systems report PSI-ER327, Probe Systems, Inc., Sunnyvale, CA, Oct. 1974.

[5] Engler, H. F., and Howard, D. H. (1985)
A compendium of analytic models for coherent and non-coherent receivers.
Technical report AFWAL-TR-85-1118, Air Force Wright Aeronautical Laboratory, Sept. 1985.

[6] Park, K. Y. (1978)
Performance evaluation of energy detectors.
IEEE Transactions on Aerospace and Electronic Systems, **AES-14** (Mar. 1978), 237–241.

[7] Dillard, R. A. (1979)
Detectability of spread-spectrum signals.
IEEE Transactions on Aerospace and Electronic Systems, **AES-15** (July 1979), 526–537.

[8] Urkowitz, H. (1967)
Energy detection of unknown deterministic signals.
Proceedings of the IEEE, **55** (Apr. 1967).

[9] DiFranco, J. V., and Rubin, W. L. (1980)
Radar Detection.
Dedham, MA: Artech House, 1980.

[10] Woodring, D., and Edell, J. D. (1977)
Detectability calculation techniques.
Report NRL 5480, Naval Research Laboratory, Washington, DC, Sept. 1977.

[11] Barton, D. K. (1969)
Simple procedures for radar detection calculations.
IEEE Transactions on Aerospace and Electronic Systems, **AES-5** (Sept. 1969).

[12] Urkowitz, H. (1973)
Closed-form expressions for noncoherent radar integration gain and collapsing loss.
IEEE Transactions on Aerospace and Electronic Systems, **AES-9** (Sept. 1973).

[13] International Mathematical Statistical Libraries (1991)
FORTRAN algorithms.
International Mathematical Statistical Libraries, Houston TX, 1991.

Converting Earth-Centered, Earth-Fixed Coordinates to Geodetic Coordinates

An improved algorithm to convert Earth-centered, Earth-fixed (ECEF) coordinates to geodetic coordinates is presented. It is faster than other methods and has accuracy equal to that of one of the most accurate existing algorithms, for heights greater than −3,000,000 m.

I. INTRODUCTION

An earlier algorithm [1], which computes an initial estimate then refines it, is improved in three ways: 1) An error at high latitudes is eliminated by using acos ( ) instead of asin ( ), 2) terms are rearranged to simplify the computation of $\sin(\phi - \phi')$, and 3) a more accurate height formula is used. The new algorithm is derived in the next section.

To estimate accuracy, a testbed program is used to determine the maximum and average output errors of the algorithm over a large number of input test points generated by the testbed program. Each geodetic test point is exactly converted to Earth-centered, Earth-fixed (ECEF) coordinates, approximately converted by the algorithm to geodetic, and exactly converted back to ECEF where magnitude of the 3-dimensional error is computed. The testbed program

Manuscript received November 4, 1994; revised May 10, 1995.

IEEE Log No. T-AES/32/1/00787.

0018-9251/96/$5.00

is coded in Borland Turbo C 3.0 long double precision (significance guaranteed through 19 digits) on a 486-DX2 66 MHz personal computer. The conversion routine (algorithm) to be tested is coded in double precision (15 significant digits). The testbed is applied to the old, the new, and one of the most accurate existing algorithms. Results are compared in the last section.

II. NEW ALGORITHM

Given ECEF coordinates x,y,z of a point P, it is desired to find geodetic latitude ϕ, longitude λ, and height h. Longitude is computed $\lambda = \text{atan}\,2(y,x)$, while latitude and height are a function of z and $w = \sqrt{x^2 + y^2}$. In this wz meridian plane, an ellipse with semimajor axis a and eccentricity e has equation $w^2/a^2 + z^2/b^2 = 1$ where $b^2 = (1 - e^2)a^2$, which imply ϕ and h are related to geocentric polar coordinates ϕ' and r by

$$w = (r_e + h)\cos\phi = r\cos\phi' \tag{1}$$

$$z = [(1 - e^2)r_e + h]\sin\phi = r\sin\phi' \tag{2}$$

where $r_e = a/\sqrt{1 - e^2\sin^2\phi}$. Note that $x = w\cos\lambda$ and $y = w\sin\lambda$.

The approach taken here is to make an initial estimate of latitude, then find precise estimates of latitude and height by geometry. Initial latitude ϕ_1 is found by way of Gersten's estimates of $\sin(\phi - \phi')$ and $\cos(\phi - \phi')$, which are obtained as follows [2]. Multiply (1) and (2) by $\sin\phi$ and $\cos\phi$, subtract, and approximate with the first two terms of the binomial series to get

$$\sin(\phi - \phi') = \frac{k\sin\phi\cos\phi}{\sqrt{1 - e^2\sin^2\phi}} \approx k\sin\phi\cos\phi[1 + (e^2/2)\sin^2\phi] \tag{3}$$

where $k = ae^2/r$. Terms with powers of e greater than 4 have been dropped. Approximate with two terms of the binomial series and substitute (3) to obtain

$$\cos(\phi - \phi') = \sqrt{1 - \sin^2(\phi - \phi')} \approx 1 - (1/2)\sin^2(\phi - \phi') \approx 1 - (1/2)k^2\sin^2\phi\cos^2\phi. \tag{4}$$

To evaluate (3) and (4), estimate $\sin\phi$ and $\cos\phi$ with accuracy through e^2 by

$$\sin\phi = \sin\phi'\cos(\phi - \phi') + \cos\phi'\sin(\phi - \phi') \approx \sin\phi' + \cos\phi'(k\sin\phi\cos\phi) \approx \sin\phi'(1 + k\cos^2\phi') \tag{5}$$

$$\cos\phi \approx \cos\phi'(1 - k\sin^2\phi') \tag{6}$$

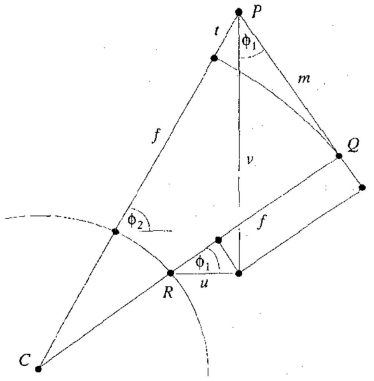

Fig. 1. Circle tangent to ellipse at R.

hence

$$\sin(\phi - \phi') \approx k\sin\phi'\cos\phi'[k + 1 - (2k - e^2/2)\sin^2\phi'] \tag{7}$$

$$\cos(\phi - \phi') \approx 1 - (k^2/2)\sin^2\phi'\cos^2\phi'. \tag{8}$$

There are several ways to use Gersten's estimates. The approach taken here is to substitute (7) and (8) into

$$\sin\phi = \sin\phi'\cos(\phi - \phi') + \cos\phi'\sin(\phi - \phi') \tag{9}$$

$$\cos\phi = \cos\phi'\cos(\phi - \phi') - \sin\phi'\sin(\phi - \phi') \tag{10}$$

to get expressions for $\sin\phi_1$ and $\cos\phi_1$

$$s_1 = s(1 + c^2(a_1 + a_2/r + s^2(a_3 - a_4/r))/r) \tag{11}$$

$$c_1 = c(1 - s^2(a_5 - a_2/r - c^2(a_3 - a_4/r))/r) \tag{12}$$

where $s = z/r$, $c = w/r$, $a_1 = ae^2$, $a_2 = a^2e^4$, $a_3 = ae^4/2$, $a_4 = (5/2)a^2e^4$ and $a_5 = a_1 + a_3$. Since the function asin ( ) is less accurate near the poles, compute s_1 by (11), $\phi_1 = \text{asin}(s_1)$ and $c_1 = \sqrt{1 - s_1^2}$ if $|\phi'| < 57°$, and c_1 by (12), $\phi_1 = \text{acos}(c_1)$ and $s_1 = \sqrt{1 - c_1^2}$ otherwise. We find $|\phi_1 - \phi| < 4.2 \times 10^{-7}$ rad for $h > -3{,}000{,}000$ m.

Precise latitude and height are now obtained. Let R be on the ellipse at latitude ϕ_1. In Fig. 1, point P has coordinates relative to R given exactly by

$$u = w - r_1c_1 \tag{13}$$

$$v = z - (1 - e^2)r_1s_1 \tag{14}$$

where $r_1 = a/\sqrt{g}$ and $g = 1 - e^2s_1^2$. Note that

$$f = c_1u + s_1v \tag{15}$$

$$m = c_1v - s_1u \tag{16}$$

and that the radius of curvature at Q is [3]

$$r_c = QC = (1 - e^2)r_1/g + f. \tag{17}$$

TABLE I
Comparison of Algorithms

Algorithm	Required Operations: cub rt	trig fun	sq rt	mul div	add sub	Set	Error: avg 10^{-9}m	max 10^{-9}m	Maximal Point: lat deg	lon deg	ht km
Old	0	1	3	31	22	1	4.8	30.0	89.9	38.	99.8
						2	6.0	368.	75.0	156.	−3000
New	0	1	3	24	14	1	0.7	2.7	64.1	149.	73.0
						2	2.1	14.1	14.0	167.	29620
Heikkinen	1	1	5	31	17	1	0.7	3.1	0.7	120.	−1.1
						2	2.0	19.7	5.0	165.	29170

Modeling the ellipse by a circle centered at C we find

$$\phi \approx \phi_2 = \phi_1 + \tan^{-1}(m/r_c) \approx \phi_1 + m/r_c \tag{18}$$

$$h \approx f + t \tag{19}$$

where

$$t = \sqrt{r_c^2 + m^2} - r_c = r_c\sqrt{1 + m^2/r_c^2} - r_c$$
$$\approx r_c[1 + m^2/(2r_c^2) - 1] = m^2/(2r_c). \tag{20}$$

C coding for (11)–(20) is shown in the Appendix. Note that no alternative computations are needed at the equator or polar axis.

III. TEST POINTS

For near-Earth testing, the points in set 1 are obtained by varying latitude from 0° to 90° by 0.1°, longitude from 0° to 180° by 1° and height from −10,000 m to 100,000 m by 100 m. Only positive latitudes are used, as the new algorithm is symmetric about the equatorial plane.

To test at extreme heights, set 2 is obtained by varying latitude by 0.5° and varying height from −3,000,000 m to 30,000,000 m by 10,000 m. We extend this region only to 3,000,000 m below the Earth's surface (half an Earth's radius) because larger errors near the geocenter would give misleading results and there is little practical interest there. The error is 0.000002 meter at $h = -5{,}000{,}000$ m.

IV. TEST RESULTS

As shown in Table I, the new algorithm is simpler and more accurate than the old algorithm [1]. Operation counts listed in the table do not include the w and longitude computations, common to all such algorithms. Since Heikkinen's algorithm is the most accurate of the seven algorithms recently tested by Zhu [4], we have coded it efficiently and tested it here, for purposes of comparison. As indicated in Table I, the new algorithm is as accurate as Heikkinen's over sets 1 and 2, but requires less computation. Timing runs show the new algorithm requires only 63% of the execution time of Heikkinen's algorithm.

APPENDIX. CODING

```
latlon (x,y,z,lat,lon,ht)/*c code*/
double x,y,z,*lat,*lon,*ht;
{
    double a = 6378137.0; /*wgs-84*/
    double e2 = 6.6943799901377997e − 3;
    double a1 = 4.2697672707157535e + 4;
    double a2 = 1.8230912546075455e + 9;
    double a3 = 1.4291722289812413e + 2;
    double a4 = 4.5577281365188637e + 9;
    double a5 = 4.2840589930055659e + 4;
    double a6 = 9.9330562000986220e − 1;
    /* a1 = a*e2, a2 = a1*a1, a3 = a1*e2/2, */
    /* a4 = (5/2)*a2, a5 = a1 + a3, a6 = 1 − e2 */
    double zp,w2,w,z2,r2,r,s2,c2,s,c,ss;
    double g,rg,rf,u,v,m,f,p;
    zp = fabs(z);
    w2 = x*x + y*y;
    w = sqrt(w2);
    z2 = z*z;
    r2 = w2 + z2;
    r = sqrt(r2);
    if (r < 100000.)
    {
        *lat = 0.;
        *lon = 0.;
        *ht = −1.e7;
        return;
    }
    *lon = atan2(y,x);
    s2 = z2/r2;
    c2 = w2/r2;
    u = a2/r;
    v = a3 − a4/r;
    if (c2 > .3)
    {
        s = (zp/r)*(1. + c2*(a1 + u + s2*v)/r);
        *lat = asin(s);
        ss = s*s;
        c = sqrt(1. − ss);
    }
    else
    {
        c = (w/r)*(1. − s2*(a5 − u − c2*v)/r);
        *lat = acos(c);
        ss = 1. − c*c;
        s = sqrt(ss);
    }
    g = 1. − e2*ss;
    rg = a/sqrt(g);
    rf = a6*rg;
    u = w − rg*c;
    v = zp − rf*s;
    f = c*u + s*v;
    m = c*v − s*u;
    p = m/(rf/g + f);
    *lat = *lat + p;
    *ht = f + m*p/2.;
    if (z < 0.)
      *lat = −*lat;
    return;
}
```

DONALD K. OLSON
Code 525100E
Naval Air Warfare Center
Weapons Division
Point Mugu, CA 93042-5001

REFERENCES

[1] Olson, D. K. (1988)
Calculation of geodetic coordinates from Earth-centered, Earth-fixed coordinates.
Journal of Guidance, Control and Dynamics, **11**, 2 (Mar.–Apr. 1988), 188–190.

[2] Gersten, R. H. (1961)
Geodetic sub-latitude and altitude of a space vehicle.
Journal of the Astronautical Sciences, **3**, 1 (Spring 1961), 28–29.

[3] Ewing, C. E., and Michael, M. M. (1970)
Introduction to Geodesy.
New York: American Elsevier, 1970.

[4] Zhu, J. (1994)
Conversion of Earth-centered, Earth-fixed coordinates to geodetic coordinates.
IEEE Transactions on Aerospace and Electronic Systems, **30**, 3 (July 1994), 957–962.

A Hybrid Estimator for the Cumulative Probability of Detection of Surveillance Radars

A hybrid estimator is formulated by combining the estimates from an empirical Bayes estimator and a jackknifed Bayes estimator. This hybrid estimator performs better than the maximum likelihood estimator, when used to estimate the cumulative probability of detection of surveillance radars.

I. INTRODUCTION

This investigation addresses the problem of estimating the cumulative probability of detection (CPD) of surveillance radars. A similar study was done in [1] in which three estimators were investigated, and the maximum likelihood estimator (MLE) was found to be the best in the minimum mean squared error (MMSE) sense. The scenario for this investigation follows closely that of [1].

The CPD is commonly used as a performance indicator for surveillance radars. Suppose a controlled experiment, comprising n repeated identical trials, is conducted to estimate the CPD of an air surveillance radar. An experiment like this is expensive and so n is usually small. Each trial requires an aircraft to approach the radar on a radial trajectory and at constant speed, starting from the maximum detection range of the radar. The start of each trial corresponds to the first scan of the radar and so, using $r(i)$ to denote the range of the aircraft at scan i, we have

$$r(1) = \text{range of aircraft at scan 1}$$
$$= \text{maximum detection range of radar.}$$

We assume that all clutter and noise processes affecting detection are independent from scan to scan. The conditions under which this assumption is approximately valid have been discussed in [1]. Let $p(i)$ denote the single-scan probability of detection (SSPD) corresponding to range $r(i)$. Then $1 - p(i)$ is the probability that the target is not detected at scan i, and $\prod_{i=1}^{m}(1 - p(i))$ is the probability that the target is not detected at any of the m scans. Therefore, the CPD of the radar at range $r(m)$, which is the probability that the radar detects the target on at least one of the m scans, is

$$P(m) = 1 - \prod_{i=1}^{m}(1 - p(i)). \tag{1}$$

A common and natural way to estimate $P(m)$ is to count the number of trials in which detections are made at or before scan m, and then to divide this number by n. This is the frequency estimator in [1] where it was pointed out that this estimator did not use all the data available from the experiment. In [1], the author proposed instead, to record the detection sequences for the n trials in an m-by-n detection matrix $D = [D_{ij}]_{1 \le i \le m, 1 \le j \le n}$ so that

$$D_{ij} = \begin{cases} 0 : \text{target was not detected at scan } i \text{ of trial } j \\ 1 : \text{target was detected at scan } i \text{ of trial } j \end{cases}$$

and then to construct estimators based on D. It was shown that the MLE which used D performed better than the frequency estimator, in the MMSE sense.

In this investigation, we construct a hybrid estimator which combines the estimates from an empirical Bayes estimator and a jackknifed Bayes estimator, and which performs better (in the MMSE sense) than the MLE. Since the MLE is known to be unbiased and uniformly minimum variance for this application, our results demonstrate the practicality of using biased estimators for achieving improved mean squared error performance.

In Section II, the forms of the frequency and MLEs are given explicitly. The Bayes estimator with uniform prior, jackknifed Bayes estimator with uniform prior, empirical Bayes estimator with unspecified prior, and hybrid estimator are also defined therein. Section III describes the Monte Carlo simulation used to compare the mean squared error performance of the estimators. The results obtained from the simulation are also presented and discussed. Finally, the findings of this investigation are summarized in Section IV.

Manuscript received February 9, 1994; revised March 27, 1995.

IEEE Log No. T-AES/32/1/00789.